Desalination and Water Treatment
www.deswater.com
doi: 10.5004/dwt.2019.23533

142 (2019) 331–340
February

Magnetized algae-silica hybrid from *Porphyridium* sp. biomass with Fe_3O_4 particle and its application as adsorbent for the removal of methylene blue from aqueous solution

Buhani[a,*], Fentri Hariyanti[a], Suharso[a,*], Rinawati[a], Sumadi[b]

[a]*Department of Chemistry, Faculty of Mathematic and Natural Sciences, University of Lampung, Jl. Soemantri Brojonegoro No. 1 Bandar, Lampung 35145, Indonesia, Tel. +62721704625; Fax: +62721702767; emails: buhani_s@yahoo.co.id (Buhani), suharso_s@yahoo.com (Suharso)*
[b]*Department of Electrical Engineering, Faculty of Engineering, University of Lampung, Jl. Soemantri Brojonegoro No. 1 Bandar, Lampung 35145, Indonesia*

Received 25 April 2018; Accepted 26 November 2018

ABSTRACT

Algae-silica (AS) hybrid material from biomass *Porphyridium* sp. has been modified by coating Fe_3O_4 particles (MPs) via a sol-gel process using tetraethyl orthosilicate to produce algae-silica-Fe_3O_4 (AS-MPs). The AS-MPs produced were applied as adsorbent for the adsorption of methylene blue (MB). Identification of functional groups was performed by infrared spectrometer indicating that in AS-MPs there were active organic groups derived from *Porphyridium* sp., silanol and siloxane. Diffraction pattern of the AS-MP material analyzed by X-ray diffraction showed that the material has higher peak intensities at 2θ = 30.04° and 35.52°. Analyst results using a particle size analyzer showed that the average particle size distribution of the AS-MP material was 1.40 μm. In addition to the results of the analysis using scanning electron microscopy, material of AS-MPs has a more heterogeneous surface morphology. The models of MB adsorption by AS and AS-MP tend to follow the pseudo-second-order kinetic model and Freundlich adsorption isotherm. The adsorption of MB solution by AS-MP produces rate constants (k_2) of 0.003 g mg^{-1} min and adsorption capacity (q_m) of 96.927 mg g^{-1} under the experimental conditions of dose of adsorbent of 2.5 mg L^{-1}, interaction pH of 6, contact time of 60 min, and temperature of 27°C. The AS-MP material obtained from the results of this study can be used as an effective adsorbent because it can remove MB dyestuff in solution, it is chemically stable in acidic and neutral media, and it can be used repeatedly.

Keywords: Porphyridium sp.; Algae-silica-magnetite hybrid; Adsorption; Methylene blue

1. Introduction

Increases in pollutants derived from coloring agents have tended to increase [1–3], especially pollutants derived from wastewater from various industrial activities that have an impact on environmental pollution. If dye is present in the wastewater, the mixture becomes more stable and more difficult to decompose due to the formation of more complex chemical structures [4]. Nearly 10,000 types of dyes with an amount of more than 7×10^5 tons are produced annually [5], and 10%–15% of these dyes are mixed in the waters [6,7], which results in environmental pollution.

One of the most widely used dyestuffs is the methylene blue (MB) dye because it is a basic substance with good solubility. The MB is a basic aniline dye with molecular formula $C_{16}H_{18}N_3SCl$. It is commonly used for dying cotton, wool, and silk. The MB dyestuff is reported to cause bad effects on humans, animals, and microorganisms as well as increase environmental pollution [8,9]. In addition, the MB dyestuff is an aromatic compound with a complex structure and difficult to degrade.

* Corresponding authors.

Therefore, it is important to control the discharge of MB dyestuff into the wastewater before being released into the environment in an effective way. One of the most appropriate ways is to process waste containing the dyestuff before it is discharged into the environment. Dye wastewater treatment can be done using adsorption method because this method is simple, relatively inexpensive, and does not generate byproducts that are harmful to the environment [10–12]. The success of the adsorption process is determined by the appropriateness of the nature and type of adsorbent used. The effective adsorbent for adsorption is the adsorbent which has a large rate and adsorption capacity, chemical stability, environmental friendly, and can be used repeatedly [13,14]. Various adsorbents such as sepiolite [15] and vermiculite [16] were successfully used to remove dyes from aqueous solution.

In general, filtration and centrifugation are used after adsorption process. They are time consuming. The blockage of filters and the loss of adsorbents may occur in filtration method. Centrifugation is not an economic method. The use of magnetic separation method offers an alternative way to solve these problems [17–20]. Currently, some researchers have developed magnetic adsorbents for the removal of the MB dyestuff from the solution. Several studies have been reported on the preparation of adsorbent and their adsorption of MB solutions, among others; material of Fe_3O_4@ MIL-100(Fe) magnetite composite [1], γ-Fe_2O_3 [2], and nanocomposite mesoporous silica [8].

In order to increase the adsorption capacity of the magnetic adsorbent, the magnetic adsorbent synthesis can be combined by adding an active group derived from algae biomass. Algae biomass is naturally an effective adsorbent for absorbing pollutants in both inorganic compounds such as heavy metals [21–23] and organic compounds derived from dyestuffs [4,14,24]. Several studies have shown that algae are alive and in the form of their biomass can adsorb chemical compounds, especially those containing cations such as metal ions and organic cations [22,24,25].

The adsorption ability of algae biomass as adsorbent can be increased by immobilizing algae biomass using various supporting polymers which are generally inorganic solids such as silica [26–29]. Enhancement of adsorption rate from adsorbate on the adsorbent was carried out using magnetite particle coating technique on silica as a biomass support matrix [30–33]. By using the technique, an adsorbent with high adsorption rate and capacity of the target compound (adsorbate) can be obtained and can quickly separate the target compound [34,35].

In this study, AS-MPs have been synthesized through a sol-gel process using tetraethyl orthosilicate (TEOS) as the precursor and organic group of *Porphyridium* sp. biomass and coated with MPs. The synthesis of this adsorbent has never been done by previous researchers. The study of the adsorption of AS-MP material on the dyestuff of MB in solution includes the effect of adsorbent dose, the adsorption kinetics and isotherms of the absorbent to the dyestuff of MB, chemical stability, and reusability of the adsorbent. The AS-MP material is effective as an adsorbent for the removal of MB dyestuff from the solution, especially for the water treatment process from MB dyestuff contaminants.

2. Experimental methods

2.1. Materials

Porphyridium sp. biomass was obtained from the Lampung Sea Cultivation Bureau (Balai Besar Budidaya Laut, Lampung), Indonesia. All chemicals used in the research were of analytical grade. Chemical reagents were purchased from Merck Co., Inc. (Germany) and consisted of TEOS, ethanol, NH_3, HCl, $FeSO_4{\cdot}4H_2O$, $FeCl_3{\cdot}6H_2O$, NaOH, MB, and CH_3COONa. The Fe_3O_4 particles (MPs) used in this study were synthesized based on procedures performed by previous researchers [33].

2.2. Preparation of AS-MPs

The AS-MP synthesis was carried out by interacting 5 mL of TEOS, 2.5 mL of distilled water, and 0.1 g of MPs in a plastic bottle by stirring for 30 min. During stirring, 1M solution of HCl up to pH ≈ 2 was added into the mixture (solution 1). In a different plastic bottle, 0.6 g *Porphyridium* sp. biomass was mixed with 5 mL of ethanol, and the mixture was stirred for 30 min (solution 2). By stirring, solution 1 was mixed with solution 2 to obtain a gel. The gel produced was left for 24 h, cleaned by water and ethanol up to the pH of filtrate was near 7, and then dried in an oven at 40°C until its weight was constant. The dried material was ground and sieved through a sieve of 200 mesh. Synthesis of AS was carried out by a similar procedure applied to yield AS-MPs, but without adding the MPs.

2.3. Characterization of the AS and AS-MPs

The synthesis resulted in a material that was characterized by an infrared (IR) spectrometer Prestige-21 Shimadzu, Japan to identify functional groups that existed in the material. The crystal structure of the material was analyzed by X-ray diffraction (XRD) (Shimadzu 6000, Japan); the surface morphology and constituent elements were investigated by scanning electron microscopy with energy dispersive X-ray spectroscopy (SEM-EDX) (Zeiss MA10, Germany). The particle size distribution of material was also investigated by particle size analyzer (Fritsch ANALYSETTE 22, Germany). Analysis of specific surface area and pore volumes was done using a surface area analyzer (Quantachrome TouchWin v1.0, U.S.A).

2.4. Batch adsorption experiment

Batch adsorption experiments were carried out to estimate the efficiency of AS and AS-MPs for the removal of MB from the artificially contaminated water. Stock solution of 1,000 mg L^{-1} of MB dyestuff was prepared by dissolving accurately weighed (1.0 g) amount of MB in 1 L of distilled water from which the solutions of desired concentrations were prepared by dilution. The adsorption process by batch method was carried out by interacting 20 mL of MB solution with the adsorbent of AS and AS-MPs stirred at 100 rpm stirring speed and temperature of 27°C to determine the effect of adsorbent dose, pH, contact time, and variation of MB solution concentration. The concentration of MB solution before and after the adsorption process was determined

using a UV-vis spectrophotometer (Agilent Cary 100, U.S.A) at a wavelength of 664 nm.

The amount of MB dyestuff adsorbed per unit mass of adsorbent and the percentage of MB adsorbed was determined using Eqs. (1)–(3).

$$q_e = \frac{(C_0 - C_e)}{m} \times V \quad (1)$$

$$q_t = \frac{(C_0 - C_t)}{m} \times V \quad (2)$$

$$R(\%) = \frac{(C_0 - C_t)}{C_0} \times 100 \quad (3)$$

where C_0 is concentration in the initial state, C_e is concentration at equilibrium, C_t is concentration at a certain time t of MB solution (mg L^{-1}), m is the mass of adsorbent (g), V is the volume of the solution (L), q is the number of MB adsorbed per unit mass (mg g^{-1}), and R is the percentage of the dyestuff of MB released.

2.5. Reusability of adsorbent

The ability to reuse AS-MP adsorbent on MB solution was studied by adsorption of MB for 5 repetitions. The adsorption was performed by interacting 50 mg of AS-MPs and 100 mg L^{-1} MB solution at pH 6, contact time of 60 min, and temperature of 27°C. Desorption of MB dyestuff adsorbed on the adsorbent was eluted using a solution of 0.1M HCl. The adsorbent regeneration was rinsed with distilled water to neutral pH and dried at 40°C for 24 h and then reused for recurrent adsorption.

2.6. Chemical stability of adsorbent

The endurance of AS-MP adsorbents in acid, neutral, and alkaline solution media was studied by interacting AS-MPs of 0.1 g into 100 mL of each solvent, i.e., 0.1M HCl solution, distilled water, and 0.1M NaOH with variation of time 1–6 d. The concentration of Si dissolved in the filtrate was analyzed using atomic absorption spectrometer (Perkins Elmer 3110, U.S.A). The percentage of Si remaining in AS-MPs was calculated based on Eq. (4).

$$\%\mathrm{Si} = \frac{[\mathrm{Si}]_t}{[\mathrm{Si}]_0} \times 100 \quad (4)$$

where $[Si]_0$ is the initial Si concentration in AS-MPs and $[Si]_t$ is the dissolved Si concentration each at time t in mg L^{-1}.

3. Results and discussion

3.1. Characterization of adsorbent

Synthesis of AS and AS-MP materials was performed through a sol-gel process using TEOS as a precursor and continued with coating by MPs. Characterization of the materials of AS and AS-MPs included functional group identification, crystalline level, particle size distribution, surface morphology, and material composition.

Identification of functional groups with IR spectroscopy has been performed to find out AS modifications that produce AS-MPs containing magnetite particles (Fig. 1). In Fig. 1(a), there are two basic characteristic peaks of MPs at around 3,300 cm^{-1} (O–H stretching) and 561 cm^{-1} derived from vibration of Fe–O indicating the existence of FeOH on MPs. In Figs. 1(b) and (c), it can be observed that the specific absorption of the silica matrix indicated in the absorption band of 462.91 cm^{-1} shows the bending vibration of the siloxane (Si–O–Si) group. The symmetrical stretching vibration of Si–O in siloxane is indicated in uptake at about 786.95 cm^{-1}. Strong absorption bands at 1,072.51 cm^{-1} indicate the asymmetric stretching vibration of Si–O from siloxane (Si–O–Si) [26]. In addition, the absorption loss at 964.40 cm^{-1} (Si–O vibration of Si–OH) is due to the reduced number of silanol groups caused by condensation of *Porphyridium* sp. algae biomass. Successful hybridization between the silica matrix and the biomass of *Porphyridium* sp. was also indicated by the appearance of absorbing bands at the wave number 2,931.80 cm^{-1}, which is the stretching vibration of the group $–CH_2$ (Figs. 1(a) and (b)) derived from *Porphyridium* sp. biomass [26]. The presence of magnetite particles in AS-MPs can be known by the appearance of uptake at 563 cm^{-1} derived from Fe–O vibrations in MPs (Fig. 1(a)) [19,20] which is also available on AS-MPs (Fig. 1(c)).

Fig. 2 displays XRD patterns of MPs, AS, and AS-MPs. From the XRD pattern, the MP (Fig. 2(a)) material was observed that there were strong diffraction peaks each at 2θ = 30.04°, 35.52°, 43.10°, 53.41°, 57.04°, and 62.62° which is the XRD pattern of a standard magnetite crystal [19,30] with spinel structure having six characteristic peaks, according to the database of Joint Committee on Powder Diffraction Standards. In the AS-MPs (Fig. 2(c)), there is a change in the amorphous structure of AS (Fig. 2(b)) because it is dominated by SiO_2, which is characterized as amorphous [35] which is marked by the appearance of several peaks with great intensities at 2θ = 30.04° and 35.52°, which are characteristic of MPs [31,36].

The effect of adding MPs on algae-silica (AS) hybrids was also studied by knowing the particle size distribution (Fig. 3).

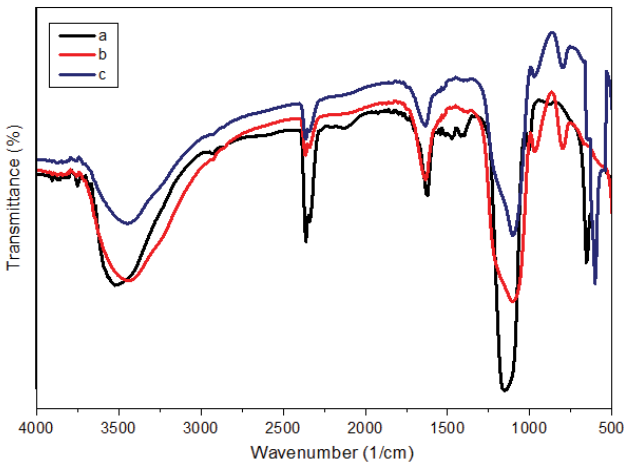

Fig. 1. Infrared spectra of the (a) MPs, (b) AS, and (c) AS-MPs.

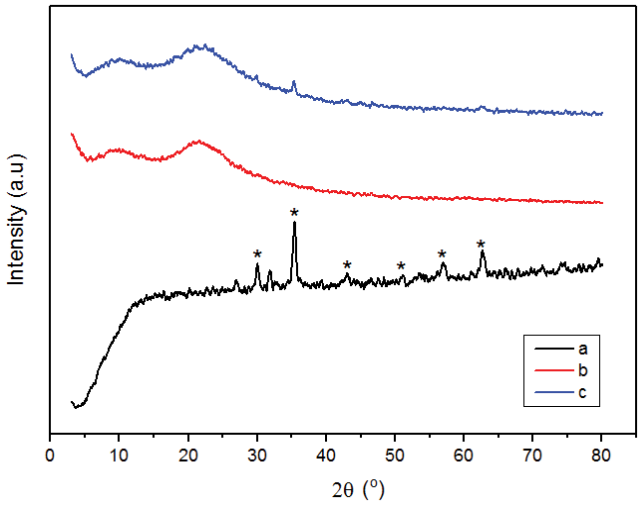

Fig. 2. XRD patterns of a) MPs, b) AS, and c) AS-MPs.

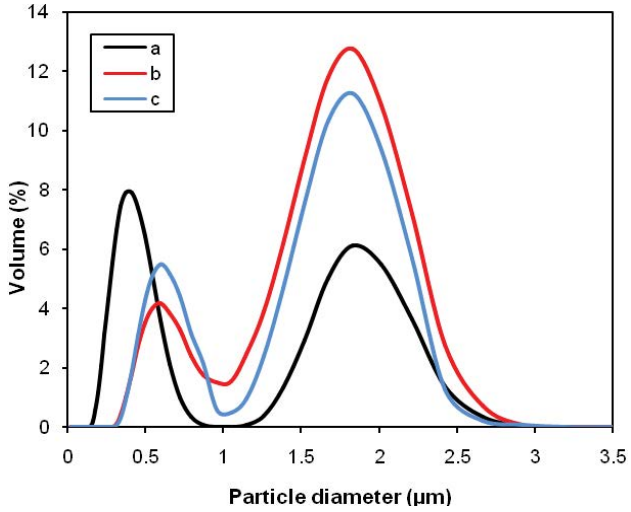

Fig. 3. Particle size distribution of (a) MPs, (b) AS, and (c) AS-MPs.

The presence of magnetite particles on AS-MPs causes a decrease in average particle size distribution. The average particle size distribution in the AS without MPs is 1.47 μm and with the MPs falling to 1.40 μm. From Fig. 3, it can also be seen that there is a decrease in percent volume for large particle diameters (1.83 μm) from 12.74% in the AS to 11.24% in AS-MPs and an increase in the percent volume of small particle size distribution (0.59 μm) in the AS by 4.17%–5.6% in AS-MPs. This suggests that the presence of MP particles causes a decrease in particle size distribution in AS-MPs. In addition, the specific surface area and pore volumes of AS and AS-MPs were determined through Brunauer–Emmett–Teller equation. The results show that there is a decrease in the specific surface areas from 170.019 for AS and 104.873 $m^2 g^{-1}$ for AS-MPs with pore volumes of 0.235 $cm^3 g^{-1}$ for AS and 0.135 $cm^3 g^{-1}$ for AS-MPs.

SEM images and energy dispersive X-ray spectroscopy (EDX) spectra from AS and AS-MPs are shown in Fig. 4. The results of surface morphology analysis with SEM show morphological differences on surface AS-MPs compared with AS, due to the presence of the magnetite particles. On the AS-MPs looks surface morphology which is more heterogeneous and contrast, this occurs because of the presence of Fe element derived from MPs while in the AS more dominated silica matrix so it is more homogeneous. The existence of MPs containing high atomic numbers in these materials causes a higher acceleration of atoms, producing a higher intensity contrast caused by broad scattering [33]. From the data EDX (Table 1) can also be known that on the AS-MPs, besides there are constituent elements derived from the silica matrix and *Porphyridium* sp. biomass, there are also other elements that come from magnetite (Fe and O) as shown in Fig. 4(b) and Table 1.

3.2. Adsorption

3.2.1. Effect of adsorbent dose

The effect of adsorbent dose of AS and AS-MPs in solution was studied using a range of adsorbent dose of 0.5–2.5 g L^{-1} (Fig. 5). The increase in adsorption on the AS starts from 20% to 75% while on AS-MPs from 35% to 90%. The data shown in Fig. 5 indicate that the more amount of doses of the adsorbent interacted the more the amount of the adsorbed MB dye. The adsorbent mass is one of the decisive factors in the adsorption process [37] because the increased concentration of adsorbent used will increase the number of active sites of adsorbent in absorbing the adsorbate. The percentage of the adsorbed MB dyestuff on AS-MPs is greater than that on the AS; this occurs because on AS-MPs, there are MPs that cause the adsorbent to be magnetic, thus increasing the number of active sites of adsorbent [33].

3.2.2. Effect of solution pH

One important factor to be considered in the adsorption process is the effect of the pH of the solution. Depending on the pH of medium, the surface can be positively, negatively, or even neutrally charged. In this study, the pH_{PZC} (point of zero charge) value used is in accordance with the results of previous studies with similar adsorbents [33]. In the process of adsorption of MB solution by AS and AS-MPs, the effect of pH was studied by varying MB solution using pH range of 2–9 (Fig. 6).

From the data contained in Fig. 6, it can be observed that the amount of MB dyestuff adsorbed increases with increasing pH of the MB solution and optimum at pH 6–8 and then begins to decrease at pH 9. Optimum condition

Table 1
Analysis results of element composition with EDX

Elements	AS		AS-MPs	
	Weight (%)	Atomic (%)	Weight (%)	Atomic (%)
Si	36.35	32.83	33.76	31.99
O	34.64	51.58	32.45	45.51
C	19.20	10.14	19.61	11.93
N	9.81	5.45	9.75	4.57
Fe	0.00	0.00	4.43	6.00
Total	100.00	100.00	100.00	100.00

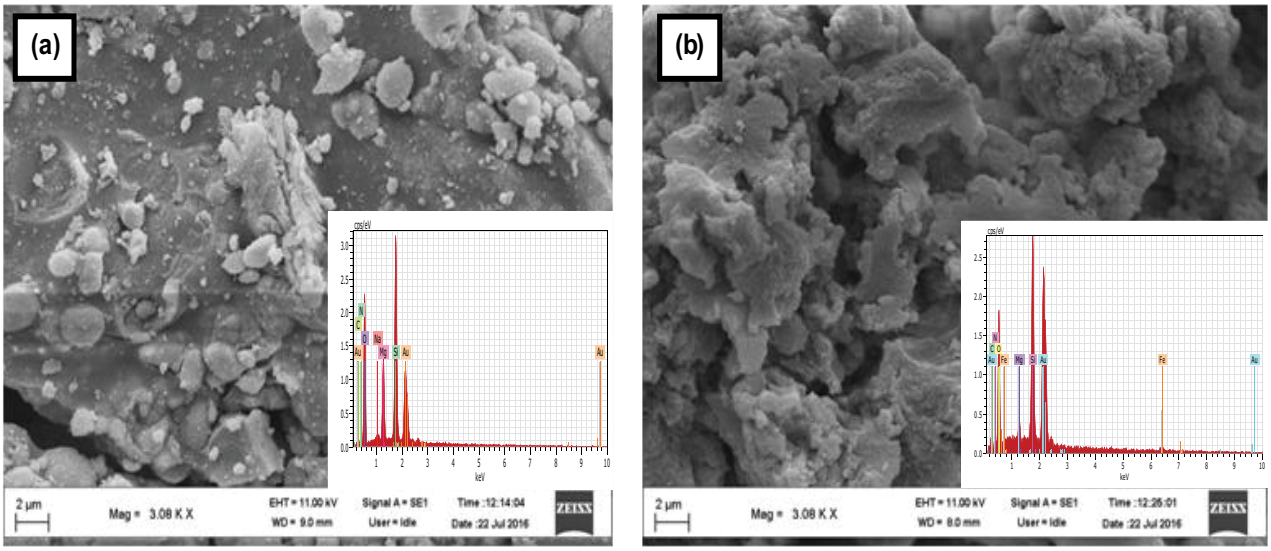

Fig. 4. SEM images and EDX spectra of (a) AS and (b) AS-MPs.

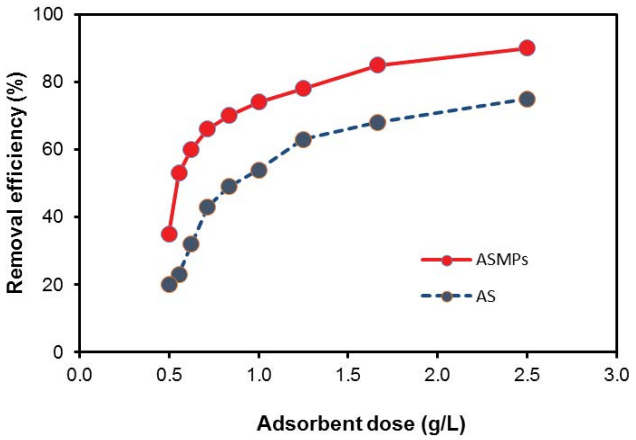

Fig. 5. Influence of adsorbent dose on MB removal yield (pH of 6, MB concentration of 100 mg L^{-1}, contact time of 60 min, temperature of 27°C, and agitation speed of 100 rpm).

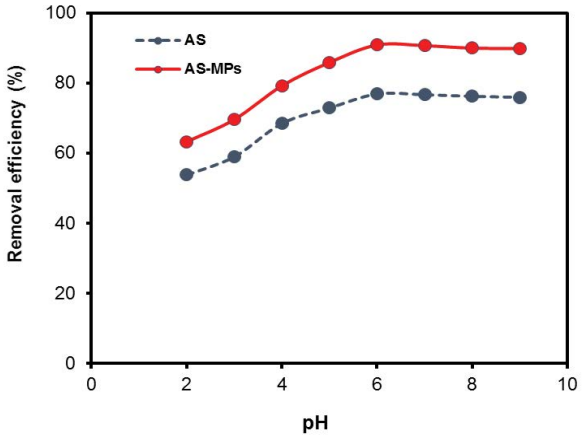

Fig. 6. Influence of pH on MB adsorption to AS and AS-MPs (contact time of 60 min, concentration of 100 mg L^{-1}, temperature of 27°C, and agitation speed of 100 rpm).

of adsorption process of MB dyestuff on AS-MPs that happened at pH 6–8 tends to be in line with the value of pH_{ZPC} determined by previous research [20,33] on the adsorbents based on silica-magnetite nanoparticle and *Tetraselmis* sp. biomass modified with silica-coated magnetite nanoparticles with the value of pH_{ZPC} 6.2 and 6.0. For medium pH above pH_{ZPC} (pH > pH_{PZC}), the adsorbent surface will be of negative charge caused by deprotonation of functional groups or adsorption of hydroxyl species. If medium pH is lower than pH_{ZPC} (pH < pH_{PZC}), the adsorbent surface will be of positive charge resulting from protonation of functional groups. As it is known, the MB dyestuff is cationic dyes that are positively charged while the adsorbents of AS and AS-MPs have functional groups such as amino, hydroxyl, and carboxyl derived from algae biomass and silanol groups that are negatively charged [21,33]. At low pH, the adsorption process is not optimal because at this pH, there is competition between the dyestuff of MB with the proton contained on the AS and AS-MP active sites. This occurs because the active groups existing on the AS and AS-MPs undergo protonation resulting in the binding of ions of hydrogen (H^+) and hydronium (H_3O^+) which will reduce the availability of the active sites in the adsorbent to interact with the cationic MB [38]. The increase in pH increases the electrostatic interaction between the cationic MB dyestuff and the negatively charged AS and AS-MP surface sites [20]. At a higher pH > 8, a decrease in adsorption begins. This is due to the formation of hydroxide species which tend to precipitate [34,39]. Besides, silica as the matrix of AS and AS-MPs is less stable at high pH [13]; consequently at this pH, the active sites on the adsorbent began to be damaged so that the adsorption of MB dyestuff decreased.

3.2.3. Influence of contact time

Influence of contact time of MB dyestuff with AS and AS-MPs was studied by interacting MB at interaction time varying from 0 to 90 min (Fig. 7). From the data contained in Fig. 7, it can be seen that generally the adsorption of the

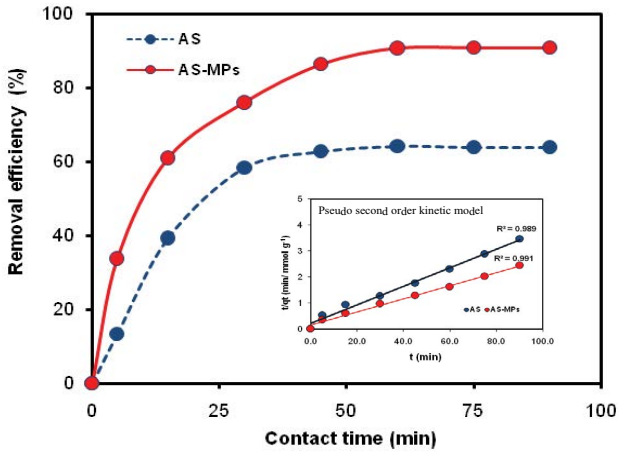

Fig. 7. Influence of contact time on adsorption of methylene blue onto AS and AS-MPs (pH of 6, MB concentration of 100 mg L^{-1}, temperature of 27°C, and agitation speed of 100 rpm).

MB dyestuff is relatively fast. In the first 15 min, adsorption increased sharply with the percentage of MB dyestuff adsorbed on the AS and the AS-MPs, respectively, being 39.27% and 60.89%; then there was an increase of adsorbed MB dyestuff, and it reached constant at 60 min interaction time, respectively, for AS and AS-MPs of 64.12% and 90.65%. At this stage, the adsorption process is estimated to have reached equilibrium and the addition of time does not give rise to the amount of MB adsorbed.

The kinetic model of the adsorption process of MB dyestuff by AS and AS-MPs is determined using the data contained in Fig. 7. The data were analyzed by kinetic models of pseudo-first order [Eq. (5)] and pseudo-second order [Eq. (6)] [8,19].

$$\log\left(q_e - q_t\right) = \log q_e - \frac{k_1}{2.303} \times t \tag{5}$$

$$\frac{t}{q_t} = \frac{1}{k_2 q_e^2} + \frac{t}{q_e} \tag{6}$$

where q_t and q_e (mg g^{-1}) are total MB dyestuff adsorption capacity at time t and at equilibrium, respectively, k_1 and k_2 are the first-order and second-order rate constants, respectively. The data of the experimental kinetics and the kinetic parameters are shown in Table 2.

From the data contained in Table 2, it can be seen that the kinetic model of MB dyestuff by the AS and AS-MPs tends to follow the pseudo-second-order kinetic model which is indicated by a higher correlation coefficient (R^2) value compared with R^2 on the pseudo-first-order kinetic model. The R^2 values of the pseudo-second-order kinetic models are 0.989 for AS and 0.991 for AS-MPs, respectively, as shown in Table 2. The good agreement between the experimental data and pseudo-second-order model can further be supported by the similar value of the experimental q_e (exp) and the calculated q_e (cal) from the kinetic equation. In Table 2, it can be seen that the pseudo-second-order adsorption rate constant (k_2) of MB by AS-MPs is larger than that of the AS. In AS-MPs, in addition, there are an active group of *Porphrydium* sp. algae biomass and the silica matrix, and the presence of MPs causes the adsorbent to be magnetic. The coating of magnetite particles on silica as an algae biomass support matrix causes an increase in the adsorption rate of the adsorbate on the adsorbent [31,32,34].

3.2.4. The influence of MB concentration

The AS and AS-MP adsorption capability in absorbing the MB dyestuff was investigated through the interaction of MB solutions at varying concentrations ranging from 0 to 250 mg L^{-1}. In Fig. 8, it can be observed that there is an increase in the number of MB dyestuff adsorbed with increasing concentration of MB dyestuff interacted. Adsorption of MB dyestuff increased sharply at low equilibrium concentrations and gradually increased at high concentrations. This shows that the AS-MPs have a high adsorption affinity

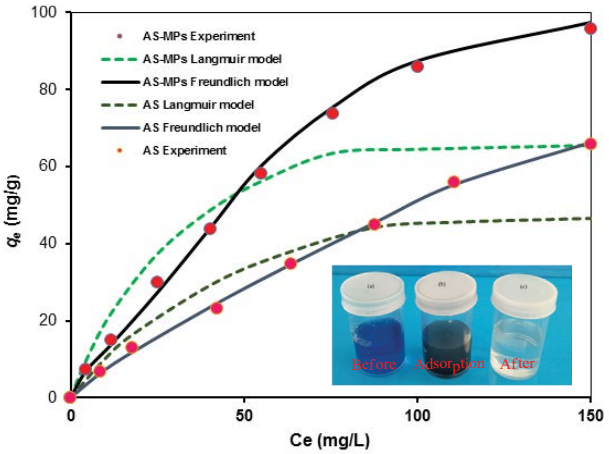

Fig. 8. Equilibrium adsorption isotherm of MB solution on AS and AS-MPs (amount of adsorbent: 2.5 g L^{-1}, pH of MB solution: 6, contact time: 60 min, temperature: 27°C, and agitation speed: 100 rpm) and photographs of selected sample before and after adsorption.

Table 2
Pseudo-first-order and pseudo-second-order rate constants for the adsorption of MB on AS and AS-MPs at temperature of 27°C and pH of 6

Adsorbents	q_e exp (mg g^{-1})	Pseudo-first order			Pseudo-second order		
		q_e cal (mg g^{-1})	k_1 (min^{-1})	R^2	q_e cal (mg g^{-1})	k_2 (g mg^{-1} min)	R^2
AS	26.097	20.208	0.085	0.874	25.641	0.002	0.989
AS-MPs	36.897	25.110	0.090	0.694	31.250	0.003	0.991

for the dyestuff of MB; blue color of MB becomes visible in the initial state before the adsorption process becomes clear after adsorption is done (Fig. 8).

In order to obtain the adsorption isotherm pattern that plays a role in describing the distribution between solution and solid phase, the data contained in Fig. 8 were analyzed using adsorption isotherm models of Langmuir [Eq. (7)] and Freundlich [Eq. (8)] [11,19,20] as follows:

$$\frac{1}{q_e} = \frac{1}{q_m K_L C_e} + \frac{1}{q_m} \tag{7}$$

$$\log q_e = \log K_F + \frac{1}{n} \log C_e \tag{8}$$

where C_e (mg L^{-1}) is the equilibrium concentration of MB solution, q_e (mg g^{-1}) is the adsorption capacity of MB at equilibrium, q_m (mg g^{-1}) is the adsorbent monolayer adsorption capacity, and K_L is the equilibrium constant including the affinity of binding sites (L mg^{-1}). K_L and q_m can be determined from the linear equation plot of log $1/q_e$ vs. $1/C_e$, which will produce a straight line with $1/q_m K_L$ as slope and $1/q_m$ as intercept. K_F ((mg g^{-1}) (L $mg^{-1})^{1/n}$) is the adsorption capacity factor and n is the adsorption intensity factor, with n values ranging from 1 to 10 [40]. Next, plot of log q_e versus log C_e will produce K_F and exponent of n.

Langmuir adsorption isotherm model assumes that on the surface of the adsorbent, there are a certain number of active sites that are proportional to the surface area, the adsorbent surface is uniform, and the adsorption process is monolayer [41,42]. While Freundlich adsorption isotherm model is an empirical equation employed for heterogeneous system and adsorption at multilayers [1].

The adsorption parameters of MB by AS and AS-MPs shown in Table 3 show that the R^2 value of the Freundlich adsorption isotherm model is higher than that of Langmuir adsorption isotherm model for adsorption of MB dyestuff both in AS and AS-MPs. This suggests that the adsorption isotherm model for MB is more fitting to the Freundlich adsorption isotherm model supported by the adsorption of the experimental results closer to the Freundlich model (Fig. 8). Similar results were reported for the adsorption isotherm of various organic pollutants onto activated carbon cloth [43–46].

Freundlich constants (n) of MB adsorption by AS and AS-MPs (Table 3) have values greater than 1; this indicates that the adsorption of MB on AS and AS-MPs is favorable in this research [2]. The MB adsorption in AS and AS-MPs not only occurs on active sites on the homogeneous (monolayer) adsorbent surface but also occurs reversibly on heterogeneous (multilayer) adsorbent surfaces [14].

The adsorption capacity of MB dyestuff by AS-MPs is larger than AS (Table 3); these data are in line with the pseudo-second-order adsorption rate constants (k_2) (Table 2). The presence of MPs in AS hybrid causes adsorbent to be magnetic thereby increasing the removal rate of MB from solution and the amount of MB adsorbed. In addition, the presence of MPs causes the particle size of AS-MPs to be smaller than that of the AS. This increases the surface area on AS-MPs so that the number of active sites will also increase [47]. Thus, it can be stated that the adsorption of MB dye on AS-MPs not only occurs chemically through the interaction of anionic active groups with cationic MB but also occurs through the physical interaction due to the influence of the magnetic properties of the adsorbent. Table 4 shows the comparison

Table 3
Langmuir and Freundlich parameters for the adsorption of MB on AS and AS-MPs at temperature of 27°C, pH of 6, and contact time of 60 min

Adsorbent	Langmuir			Freundlich		
	q_m (mg g^{-1})	K_L (L mg^{-1}) x 10^{-2}	R^2	K_F (mg g^{-1}) (L $mg^{-1})^{1/n}$	n	R^2
AS	78.015	4.801	0.739	1.183	1.231	0.997
AS-MPs	96.927	8.009	0.844	4.842	1.618	0.993

Table 4
Comparison of maximum adsorption capacity of MB on various adsorbents

Adsorbent	q_m (mg g^{-1})	Experimental condition (pH and temperature)	Reference
Magnetite Porous metal–organic frameworks (MOFs)	20.20	– and 25°C	[48]
Carbon nanotubes	35.40	7.0°C and 25°C	[49]
Magnetite-loaded multiwalled carbon nanotubes	48.06	6.0°C and 25°C	[50]
γ-Fe_2O_3	51.71	6.6°C and 25°C	[2]
Kaolin	72.57	9.0°C and 25°C	[51]
Fe_3O_4@MIL-100(Fe) magnetite composite	73.80	9.0°C and 45°C	[1]
Activated carbon	82.90	7.0°C and 25°C	[52]
Silica-polymer hybrid	87.37	7.0°C and 25°C	[38]
AS-MPs	96.93	6.0°C and 27°C	This study

of the maximum adsorption capacity (q_m) of AS-MPs to the dyestuff of MB with some other adsorbents on the previously reported MB dyestuff.

3.3. Reusability of adsorbent

The reuse of AS-MPs as adsorbent of MB solution was studied by conducting adsorption-desorption process for 5 repetitions (Fig. 9). The result of adsorption of MB solution and desorption with 0.1M HCl eluent solution repeatedly for 4 repetitions did not significantly decrease the adsorption capacity of MB. The HCl solution is effective as an eluent to release MB dyestuff from the adsorbent through the substitution of proton against the MB dyestuff as the organic cation [13]. The AS-MP reuse data are an important aspect in wastewater treatment handling as it is very important in reducing water treatment costs.

3.4. Chemical stability of adsorbent

The endurance of the AS-MP adsorbent in the medium of acidic, alkaline, and neutral solutions was known by

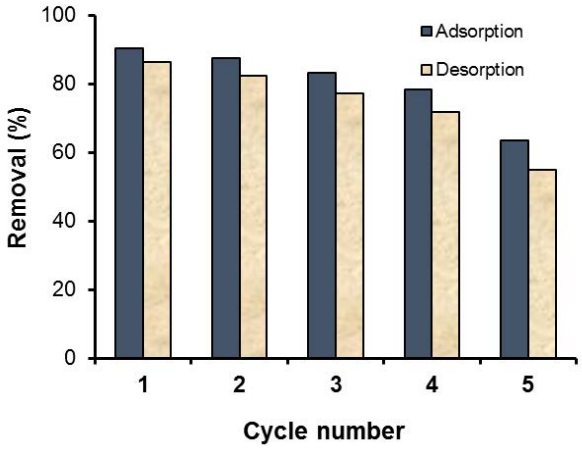

Fig. 9. Reusability number efficiency of the adsorption-desorption process of MB on AS-MPs.

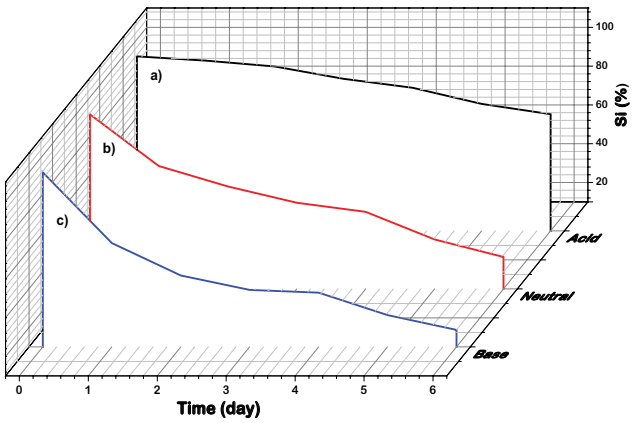

Fig. 10. The relationship between the interaction time and % [Si] remaining on AS-MPs in the solution medium of (a) 0.1M HCl, (b) distilled water, and (c) 0.1M NaOH.

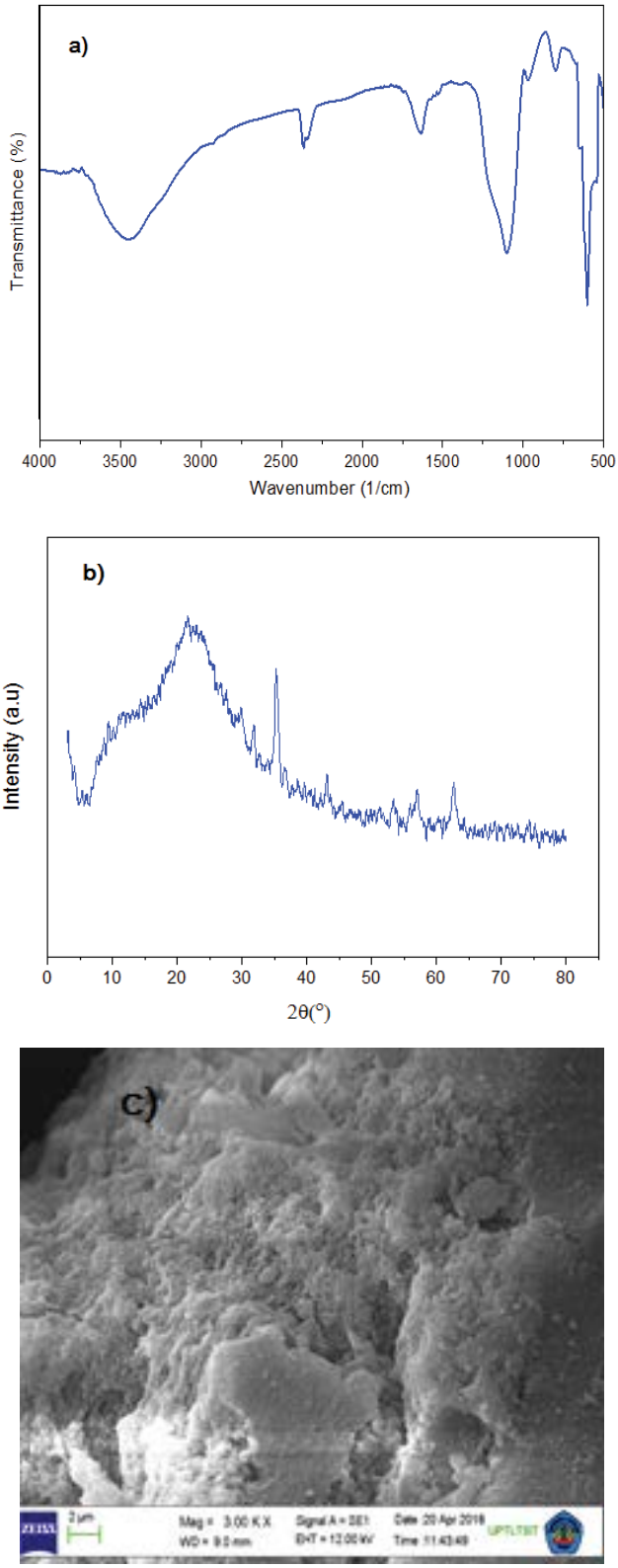

Fig. 11. (a) IR spectrum, (b) XRD pattern, and(c) SEM image of AS-MPs after adsorption process of MB solution (amount of adsorbent: 2.5 g L^{-1}, solution pH of MB: 6, contact time: 60 min, temperature: 27°C, and agitation speed: 100 rpm).

interacting the material with 0.1M HCl, water, and 0.1M NaOH for 6 d (Fig. 10). In Fig. 10, it can be seen that the amount of Si remaining until 6 d of interaction time is at most for the acid solution medium; this indicates that the material is very stable under acidic conditions. Protonation of active groups such as –COOH, $–NH_2$, and –OH groups in AS-MP material significantly increases the stability of the material in the water medium, since the protonation limits contact between water and AS-MPs [53,54]. At the base conditions, the remaining Si concentration is at least corresponding to the increase in interaction time occurring in the aqueous solution with a fairly alkaline pH (pH < 10). The amount of dissolved Si is derived from the hydrolysis of silica network with the release of the active groups, due to the hydrolysis of the chemical bond between the organosilane and the silica surface. If the remaining Si concentration data are an indication of the stability of AS-MP material, then it can be stated that the acid-base media conditions determine the stability of the material.

Stability of AS-MPs after adsorbing MB was studied by characterizing AS-MP adsorbent using IR spectrometer, XRD, and SEM as displayed in Fig. 11. From Fig. 11, it can be observed that the characteristics of the AS-MP adsorbent have not changed in the functional groups (Fig. 11(a)), XRD diffractogram pattern (Fig. 11(b)), surface morphology of the AS-MPs (Fig. 11(c)) compared with the characteristics of AS-MPs before the adsorption process as discussed in section 3.1. These facts show that the adsorbent has stability to be reused for several times in the adsorption process of MB.

4. Conclusions

Modification of AS hybrids derived from *Porphyridium* sp. algae biomass with the MP coating has produced an effective adsorbent to remove MB dyestuff in solution. Characterization of AS-MP material shows some active groups acting as active sites for binding of the cationic MB dyestuff. The MP coating increases the rate and capacity of the AS hybrid adsorption to MB dyestuff in solution. Thus, AS-MP is an effective adsorbent for removing MB dyestuff in solution, chemically stable to acidic and neutral media, and having good reusability; so it can be applied to the processing of wastewater-containing dyestuffs such as MB.

Acknowledgement

The authors would like to thank the Directorate of Research and Community Service, Directorate General for Research and Development, Ministry of Research, Technology and Higher Education of the Republic of Indonesia who have funded this research in accordance with contract number 062/SP2H/LT/DPRM/2018 and international seminar funds in 2018. The authors give a high appreciation to Technical Service Unit of the Integrated Laboratory and the Technology Innovation Center–University of Lampung (UPT Laboratorium Terpadu dan Sentra Inovasi Teknologi–Universitas Lampung).

References

[1] Y. Shao, L. Zhou, C. Bao, J. Ma, M. Liu, F. Wang, Magnetic responsive metal–organic frameworks nanosphere with core–shell structure for highly efficient removal of methylene blue, Chem. Eng. J., 283 (2016) 1127–1136.
[2] A. El-Qanni, N.N. Nassar, G. Vitale, A. Hassan, Maghemite nanosorbcats for methylene blue adsorption and subsequent catalytic thermo-oxidative decomposition: computational modeling and thermodynamics studies, J. Colloid Interface Sci., 461 (2016) 396–408.
[3] J. Fu, Q. Xin, X. Wu, Z. Chen, Y. Yan, S. Liu, M. Wang, Q. Xu, Selective adsorption and separation of organic dyes from aqueous solution on polydopamine microspheres, J. Colloid Interface Sci., 461 (2016) 292–304.
[4] E. Daneshvar, A. Vazirzadeh, A. Niazi, M. Kousha, M. Naushad, A. Bhatnagar, Desorption of Methylene blue dye from brown macro alga: effects of operating parameters, isotherm study and kinetic modeling, J. Clean. Prod., 152 (2017) 443–453.
[5] A. Celekli, H. Bozkurt, Predictive modeling of an azo metal complex dye sorption by pumpkin husk, Environ. Sci. Pollut. Res., 20 (2013) 7355–7366.
[6] X.X. Liu, W.P. Gong, J. Luo, C.T. Zou, Y. Yang, S.J. Yang, Selective adsorption of cationic dyes from aqueous solution by polyoxometalate-based metalorganic framework composite, Appl. Surf. Sci., 362 (2016) 517–524.
[7] S. Agarwal, V.K. Gupta, M. Ghasemi, J. Azimi-Amin, *Peganum harmala*-L Seeds adsorbent for the rapid removal of noxious brilliant green dyes from aqueous phase, J. Mol. Liq., 231 (2017) 296–305.
[8] S. Kittappa, S. Pichiah, J.R. Kim, Y. Yoon, S.A. Snyder, M. Jang, Magnetized nanocomposite mesoporous silica and its application for effective removal of methylene blue from aqueous solution, Sep. Purif. Technol., 153 (2015) 67–75.
[9] S. Dardouri, J. Sghaier, A comparative study of adsorption and regeneration with different agricultural wastes as adsorbents for the removal of methylene blue from aqueous solution, Chin. J. Chem. Eng., 25 (2017) 1282–1287.
[10] J. Shu, R. Liu, H. Wu, Z. Liu, X. Sun, C. Tao, Adsorption of methylene blue on modified electrolytic manganese residue: kinetics, isotherm, thermodynamics and mechanism analysis, J. Taiwan Inst. Chem. Eng., 82 (2018) 351–359.
[11] Buhani, Narsito, Nuryono, E.S. Kunarti, Suharso, Adsorption competition of Cu(II) ion in ionic pair and multi-metal solution by ionic imprinted amino-silica hybrid adsorbent, Desal. Wat. Treat., 55 (2015) 1240–1252.
[12] Suharso, Buhani, Biosorption of Pb (II), Cu (II) and Cd (II) from aqueous solution using cassava peel waste biomass, Asian J. Chem., 23 (2011) 1112–1116.
[13] Buhani, Suharso, Z. Sembiring, Immobilization of *Chetoceros* sp microalgae with silica gel through encapsulation technique as adsorbent of Pb metal from solution, Orient. J. Chem., 28 (2012) 271–278.
[14] U.A. Guler, M. Ersan, E. Tuncel, F. Dügenci, Mono and simultaneous removal of crystal violet and safranin dyes from aqueous solutions by HDTMA-modified *Spirulina sp*., Process Saf. Environ. Prot., 99 (2016) 194–206.
[15] O. Duman, S. Tunç, T.G. Polat, Adsorptive removal of triarylmethane dye (Basic Red 9) from aqueous solution by sepiolite as effective and low-cost adsorbent, Microporous Mesoporous Mater., 210 (2015) 176–184.
[16] O. Duman, S. Tunç, T.G. Polat, Determination of adsorptive properties of expanded vermiculite for the removal of C. I. Basic Red 9 from aqueous solution: kinetic, isotherm and thermodynamic studies, Appl. Clay Sci., 109–110 (2015) 22–32.
[17] O. Duman, S. Tunç, T.G. Polat, B.K. Bozoğlan, Synthesis of magnetic oxidized multiwalled carbon nanotube-κ-carrageenan-Fe_3O_4 nanocomposite adsorbent and its application in cationic methylene blue dye adsorption, Carbohydr. Polym., 147 (2016) 79–88.
[18] O. Duman, S. Tunç, B.K. Bozoğlan, T.G. Polat, Removal of triphenylmethane and reactive azo dyes from aqueous solution by magnetic carbon nanotube-κ-carrageenan-Fe_3O_4 nanocomposite, J. Alloys Compd., 687 (2016) 370–383.
[19] S.H. Araghi, M.H. Entezari, Amino-functionalized silica magnetite nanoparticles for the simultaneous removal of pollutants from aqueous solution, Appl. Surf. Sci., 333 (2015) 68–77.

[20] M.H.P. Wondracek, A.O. Jorgetto, A.C.P. Silva, J.R. Ivassechen, J.F. Schneider, M.J. Saeki, V.A. Pedrosa, W.K. Yoshito, F. Colauto, W.A. Ortiz, G.R. Castro, Synthesis of mesoporous silica-coated magnetic nanoparticles modified with 4-amino-3-hydrazino-5-mercapto-1,2,4-triazole and its application as Cu(II) adsorbent from aqueous samples, Appl. Surf. Sci., 367 (2016) 533–541.
[21] Buhani, Musrifatun, D.S. Pratama, Suharso, Rinawati, Modification of *Chaetoceros* sp. biomass with silica-magnetite coating and adsorption studies towards Cu(II) ions in single and binary system, Asian J. Chem., 29 (2017) 2734–2739.
[22] M.M. Montazer-Rahmati, P. Rabbani, A. Abdolali, A.R. Keshtkar, Kinetics and equilibrium studies on biosorption of cadmium, lead, and nickel ions from aqueous solutions by intact and chemically modified brown algae, J. Hazard. Mater., 185 (2011) 401–407.
[23] A.K. Zeraatkar, H. Ahmadzadeh, A.F. Talebi, N.R. Moheimani, M.P. McHenry, Potential use of algae for heavy metal bioremediation, a critical review, J. Environ. Manage., 181 (2016) 817–831.
[24] R. Angelova, E. Baldikova, K. Pospiskova, Z. Maderova, M. Safarikova, I. Safarik, Magnetically modified Sargassum horneri biomass as an adsorbent for organic dye removal, J. Clean. Prod., 137 (2016) 189–194.
[25] C.E. Flores-Chaparro, L.F.C. Ruiz, M.C.A. de la Torre, M.A. Huerta-Diaz, J.R. Rangel-Mendez, Biosorption removal of benzene and toluene by three dried macro algae at different ionic strength and temperatures: algae biochemical composition and kinetics, J. Environ. Manage., 193 (2017)126–135.
[26] Buhani, Suharso, Sumadi, Adsorption kinetics and isotherm of Cd(II) ion on *Nannochloropsis* sp. biomass imprinted ionic polymer, Desalination, 259 (2010) 140–146.
[27] M.F. Desimone, C. Hélary, G. Mosser, M.M. Giraud-Guille, J. Livage, T. Coradin, Fibroblast encapsulation in hybrid silica–collagen hydrogels, J. Mater. Chem., 20 (2010) 666–668.
[28] M.V. Tuttolomondo, G.S. Alvarez, M.F. Desimone, L.E. Diaz, Removal of azo dyes from water by sol–gel immobilized *Pseudomonas* sp., J. Environ. Chem. Eng., 2 (2014) 131–136.
[29] L.R. Martins, J.A.V. Rodrigues, O.F.H. Adarme, T.M.S. Melo, L.V.A. Gurgel, L.F. Gil, Optimization of cellulose and sugarcane bagasse oxidation: application for adsorptive removal of crystal violet and auramine-O from aqueous solution, J. Colloid Interface Sci., 494 (2017) 223–241.
[30] Y. Lin, H. Chen, K. Lin, B. Chen, C. Chiou, Application of magnetic modified with amino groups to adsorb copper ion in aqueous solution, J. Environ. Sci., 23 (2011) 44–50.
[31] Q. Peng, Y. Liu, G. Zeng, W. Xu, C. Yang, J. Zhang, Biosorption of copper(II) by immobilizing *Saccharomyces cerevisiae* on the surface of chitosan-coated magnetic nanoparticle from aqueous solution, J. Hazard. Mater., 177 (2010) 676–682.
[32] S. Ghosh, A.Z.M. Badruddoza, K. Hidajat, M.S. Uddin, Adsorptive removal of emerging contaminants from water using superparamagnetic Fe_3O_4 nanoparticles bearing aminated β-cyclodextrin, J. Environ. Chem. Eng., 1 (2013) 122–130.
[33] Buhani, Rinawati, Suharso, D.P. Yuliasari, S.D. Yuwono, Removal of Ni(II), Cu(II), and Zn(II) ions from aqueous solution using *Tetraselmis* sp. biomass modified with silica-coated magnetite nanoparticle, Desal. Wat. Treat., 80 (2017) 203–213.
[34] Y. Lin, H. Chen, K. Lin, B. Chen, C. Chiou, Application of magnetic particles modified with amino groups to adsorb cooper ions in aqueous solution, J. Environ. Sci., 23 (2011) 44–50.
[35] H. Hu, Z. Wang, L. Pan, Synthesis of monodisperse Fe_3O_4 @ silica core–shell microspheres and their application for removal of heavy metal ions from water, J. Alloys Compd., 492 (2010) 656–661.
[36] A.M. Donia, A.A. Atia, F.I. Abouzayed, Preparation and characterization of nano-magnetic cellulose with fast kinetic properties towards the adsorption of some metal ions, Chem. Eng. J., 191 (2012) 22–30.
[37] R. Noroozi, T.J. Al-Musawi, H. Kazemian, E.M. Kalhori, M. Zarrabi, Removal of cyanide using surface-modified Linde Type-A zeolite nanoparticles as an efficient and eco-friendly material, J. Water Process Eng., 21 (2018) 44–51.
[38] H.S. Jamwal, S. Kumari, G.S. Chauhan, N.S. Reddy, J.H. Ahn, Silica-polymer hybrid materials as methylene blue adsorbents, J. Environ. Chem. Eng., 5 (2017) 103–113.
[39] V.K. Gupta, A. Rastogi, A. Nayak, Biosorption of nickel onto treated alga (*Oedogonium hatei*): application of isotherm and kinetic models, J. Colloid Interface Sci., 342 (2010) 533–539.
[40] Y.S. Ho, J.F. Porter, G. McKay, Equilibrium isotherm studies for the sorption of divalent metal ions onto peat: copper, nickel, and lead single component systems, Water Air Soil Pollut., 141 (2002) 1–33.
[41] X. Xin, Q. Wei, J. Yang, L. Yan, R. Feng, G. Chen, B. Du, H. Li, Highly efficient removal of heavy metal ions by amine-functionalized mesoporous Fe_3O_4 nanoparticles, Chem. Eng. J., 184 (2012) 132–140.
[42] I. Larraza, M. Lŏpez-Gŏnzales, T. Corrales, G. Marcelo, Hybrid materials: magnetite-ployethyenimine-montromolillonite, as magnetic adsorbents for Cr(VI) water treatment, J. Colloid Interface Sci., 385 (2012) 24–33.
[43] O. Duman, E. Ayranci, Structural and ionization effects on the adsorption behaviors of some anilinic compounds from aqueous solution onto high-area carbon-cloth, J. Hazard. Mater., 120 (2005) 173–181.
[44] O. Duman, E. Ayranci, Adsorption characteristics of benzaldehyde, sulphanilic acid, and p-phenolsulfonate from water, acid, or base solutions onto activated carbon cloth, Sep. Sci. Technol., 41 (2006) 3673–3692.
[45] O. Duman, E. Ayranci, Attachment of benzo-crown ethers onto activated carbon cloth to enhance the removal of chromium, cobalt and nickel ions from aqueous solutions by adsorption, J. Hazard. Mater., 176 (2010) 231–238.
[46] O. Duman, E. Ayranci, Adsorptive removal of cationic surfactants from aqueous solutions onto high-area activated carbon cloth monitored by in situ UV spectroscopy, J. Hazard. Mater., 174 (2010) 359–367.
[47] S. Shakoor, A. Nasa, Adsorptive treatment of hazardous methylene blue dye from artificially contaminated water using Cucumis sativus peel waste as a low-cost adsorbent, Groundw. Sustain. Dev., 5 (2017) 152–159.
[48] J. Zheng, C. Cheng, W.-J. Fang, C. Chen, R.-W. Yan, H.-X. Huai, C.-C. Wang, Surfactant-free synthesis of a Fe_3O_4@ZIF-8 core–shell heterostructure for adsorption of methylene blue, Cryst. Eng. Comm., 16 (2014) 3960–3964.
[49] Y.J. Yao, F.F. Xu, M. Chen, Z.X. Xu, Z.W. Zhu, Adsorption behavior of methylene blue on carbon nanotubes, Bioresour. Technol., 101 (2010) 3040–3046.
[50] L. Ai, C. Zhang, F. Liao, Y. Wang, M. Li, L. Meng, Removal of methylene blue from aqueous solution with magnetite loaded multi-wall carbon nanotube: kinetic, isotherm and mechanism analysis, J. Hazard. Mater., 198 (2011) 282–290.
[51] L. Mouni, L. Belkhiri, J.-C. Bollinger, A. Bouzaza, A. Assadi, A. Tirri, F. Dahmoune, K. Madani, H. Remini, Removal of methylene blue from aqueous solutions by adsorption on kaolin: kinetic and equilibrium studies, Appl. Clay Sci., 153 (2018) 38–45.
[52] M. Ghaedi, M.D. Ghazanfarkhani, S. Khodadoust, N. Sohrabi, M. Oftade, Acceleration of methylene blue adsorption onto activated carbon prepared from dross licorice by ultrasonic: equilibrium, kinetic and thermodynamic studies, J. Ind. Eng. Chem., 20 (2014) 2548–2560.
[53] Buhani, Suharso, Aprilia L., Chemical stability and adsorption selectivity on Cd^{2+} ionic imprinted *Nannochloropsis* sp. material with silica matrix from tetraethyl orthosilicate, Indo. J. Chem., 12 (2012) 94–99.
[54] M. Etienne, A. Walcarius, Analytical investigation of chemical reactivity and stability of aminopropyl-grafted silica in aqueous medium, Talanta, 59 (2003) 1173–1188.